

New Autonomous Decentralized Structure Formation Based on Huygens' Principle and Renormalization for Mobile Ad Hoc Networks

Kenji Takagi
Graduate School of System Design,
Tokyo Metropolitan University
Tokyo, Japan
Email: kenji.takagi.tmu@gmail.com

Chisa Takano
Graduate School of Information Sciences,
Hiroshima City University
Hiroshima, Japan
Email: takano@hiroshima-cu.ac.jp

Masaki Aida
Graduate School of System Design,
Tokyo Metropolitan University
Tokyo, Japan
Email: aida@tmu.ac.jp

Makoto Naruse
National Institute of Information
and Communications Technology (NICT)
Tokyo, Japan
Email: naruse@nict.go.jp

Abstract—This paper proposes an autonomous distributed algorithm that can construct spatial structures for clustering in mobile ad hoc networks. Since the topology of a mobile ad hoc network changes frequently, a fast, light-weight, and autonomous clustering mechanism is required. However, existing autonomous clustering mechanisms are based on differential equations and thus demand a lot of calculations for generating the spatial structures that yield clustering. This paper proposes an autonomous clustering algorithm that is based on Huygens' principle and renormalization. The most remarkable characteristics of our proposed scheme are light calculation loads and fast convergence on the cluster structures. We verify the basic characteristics of the proposed scheme. In addition, we introduce an algorithm to control the number of generated clusters in the framework of the proposed scheme by introducing a logarithmic representation of network state.

Keywords—Mobile ad hoc network, Autonomous decentralized control, Clustering, Huygens' principle, Renormalization.

I. INTRODUCTION

This paper is an extended version of the paper presented at COLLA2013 [1]. The significant progress of this paper from the earlier version is that we can control the number of cluster even if we cannot know the network state and its metric in advance. Details are explained in the body of this paper.

In large-scale communication networks, hierarchical architectures are effective for scalable network control. Let us consider how hierarchical structure can be introduced into networks. For the case of fixed networks, we can set the desired hierarchical structure at the time of designing the networks. However, this is not possible for mobile networks since their topology changes dynamically. A typical example the mobile ad hoc network (MANET) [2]. A MANET consists of mobile terminals that work as routers. That is, each terminal offers routing functions and data forwarding functions. Two terminals can directly communicate if their coverage areas of wireless communications overlap. If the areas do not overlap, the terminals communicate but relaying data through the terminals

between them, they can establish multihop communications. To achieve multihop communications, routing is one of most important issues in MANETs.

The most primitive route finding approach is called flooding [3]. In flooding, the sender terminal sends route finding packets to all adjacent terminals, which resend them to all their adjacent terminals until at least one copy of the packet reaches the destination terminal. The total amount of route finding packets sent in MANETs increases exponentially with network size (the number of terminals). It is known as the broadcast storm problem [4]. So one of the challenges in MANETs, realizing scalable routing control [5][6], is best addressed by setting a hierarchical structure through clustering [7][8].

Hereafter, we call a MANET terminal a node. An autonomous clustering mechanism for generating a hierarchical structure must offer several characteristics, as follows:

- Each node acts autonomously based on local information about its neighboring nodes.
- The generated cluster structure should reflect the state information of the network (e.g., battery power of nodes).
- The generated cluster structure should be flexible so that it can adapt to the dynamic environment.
- The convergence time of clustering should be sufficiently shorter than the timescale of topology change caused by node movement. This is because clustering should dynamically adapt to the network topology.
- Action rules of each node should be as simple as possible in order to reduce the battery power consumed by computation or processing at the node.

Since MANETs are expected to be an effective communication tool after serious disasters, the above requirements are essential for realizing clustering in ad hoc networks.

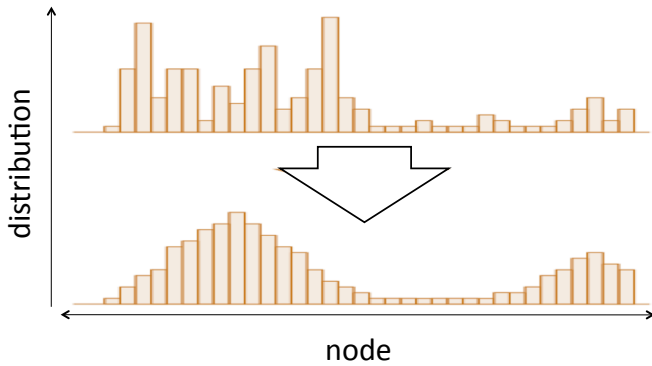


Figure 1. Concept of cluster forming.

Neglia et al. proposed a clustering mechanism based on reaction-diffusion equations [9]. Let us call it the bio-inspired approach. This is an application of Turing patterns and satisfies the first requirement listed above. Takano et al. has proposed a clustering mechanism based on the Fokker-Planck equation and includes the drift motion given by back-diffusion [10][11][12]. Let us call it the back-diffusion based approach. The back-diffusion based approach satisfies the first two requirements listed above. In addition, Hamamoto et al. recently propose a mechanism that guarantees the asymptotic stability of the cluster structure generated by the back-diffusion based approach; they showed that their mechanism can satisfy the first three requirements listed above [13].

The guarantee mechanism of asymptotic stability, in particular, implies the possibility of new autonomous clustering mechanisms. Specifically, we might be able to make a new clustering algorithm that satisfies all the requirements listed above by replacing the back-diffusion algorithm with a simple and fast-converging rule. This is because the guarantee mechanism of asymptotic stability does not depend on details of the clustering mechanism. In this paper, we use Huygens' principle as the simple and fast-converging rule, and propose a new clustering mechanism that satisfies all the requirements listed above.

The paper is organized as follows: Section II explains the concept of cluster formation and the guarantee mechanism of asymptotic stability, which is the foundation of this research. Section III proposes an autonomous clustering mechanism based on Huygens' principle. Section IV shows cluster structures generated by our proposed scheme using numerical examples and verifies that they reflect the network condition. Section V introduces an algorithm to control the number of generated clusters in the framework of the proposed scheme by introducing a logarithmic representation of network state. In addition, we show a control method of the number of clusters. The conclusion is discussed in Section VI.

II. PRELIMINARY

This section shows the framework of autonomous decentralized clustering and the related mechanism to stabilize the cluster structure.

A. Concept of Cluster Formation

In our clustering model, each node has a certain value and cluster formation is conducted by the distribution of the values of nodes. The initial value is determined by considering a certain network metric (e.g., battery power of each node). The clustering algorithm extracts a coarse grained spatial structure from the initial distribution of the values and this procedure corresponds to clustering. Figure 1 shows an example of cluster formation in a simple 1-dimensional network. The horizontal axis represents node position, and the vertical axis represents the value of the distribution for each node. The upper-half of Figure 1 represents the initial distribution, which reflects a certain network state. The lower-half of Figure 1 represents the generated coarse grained spatial structure. Each peak of the coarse grained distribution corresponds to the center of a cluster, and cluster structures reflect the initial condition.

The back-diffusion based approach is an example of this mechanism, and has a relatively faster convergence rate than the bio-inspired approach [14]. However, this clustering mechanism does not consider change from the initial condition, and so cannot adapt to the dynamic environment common to MANETs. That is why this mechanism does not satisfy the third requirement listed in the previous section.

B. Guarantee mechanism of Asymptotic Stability

To adapt the spatial structure to dynamic environments, the guarantee mechanism of the asymptotic stability of cluster structures was proposed by Hamamoto et al. [13]. In this mechanism, cluster structure generation can adapt to changes in network state; the mechanism generates stable spatial structures if the network state is fixed. As an alternative approach, Takayama et al. proposed the self-adjustment approach to stabilize the cluster structure [15]. However, it has a restriction that is applicable only to the back-diffusion based clustering. Thus, we focus on [13] in this paper.

Let us consider a one-dimensional network model for simplicity, and let $q(i, t)$ be the distribution value at node position i at time t . The distribution value, $q(i, t)$, determines the cluster structure. As an example, the initial condition $q(i, 0)$ and cluster structure $q(i, t)$ obtained at time t are shown in Figure 1. The conventional back-diffusion based approach described in Takano et al. [12] presents a rule that governs the temporal evolution of the distribution, $q(i, t)$. However, as shown in the previous section, it is difficult to guarantee the stability of $q(i, t)$ for large t . In other words, the cluster structure is not stable in a dynamic environment.

Let us consider discrete time t_k ($k = 1, 2, \dots$), and distribution $q(i, t_k)$. Since we need an autonomous decentralized algorithm, the temporal evolution of distribution $q(i, t_k)$ is determined by its local information. By introducing the temporal evaluation operator of \mathcal{T} , the temporal evolution is formally described as

$$q(i, t_{k+1}) = \mathcal{T}(q(i-1, t_k), q(i, t_k), q(i+1, t_k)). \quad (1)$$

This rule states that the distribution of node i at the next time is completely determined by the values of the present distribution at node i and its adjacent nodes.

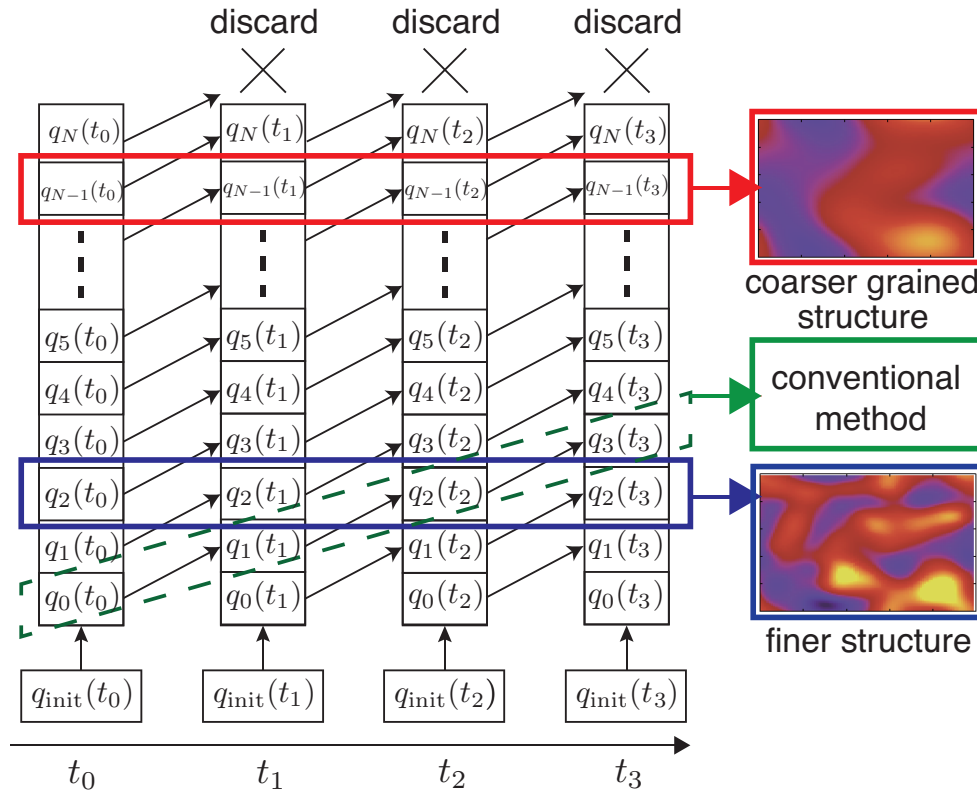


Figure 2. Outline of the guarantee mechanism of asymptotic stability.

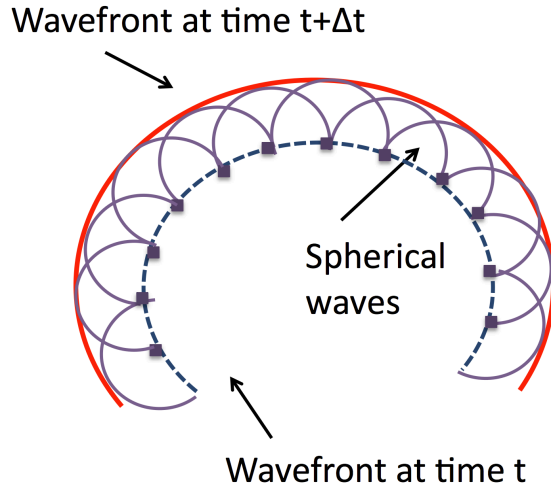


Figure 3. Example of wave propagation obeying Huygens' principle.

To guarantee asymptotic stability, we consider a vector of the distribution. Each node i has the following $N + 1$ dimensional vector

$$\mathbf{q}(i, t_k) = \{q_0(i, t_k), q_1(i, t_k), \dots, q_N(i, t_k)\}. \quad (2)$$

Here, we define the rule for the temporal evolution of the vector $\mathbf{q}(i, t_k)$. Let $q_{\text{init}}(i, t_k)$ be the distribution describing

the network state at time t_k . Then we set

$$q_0(i, t_{k+1}) = q_{\text{init}}(i, t_{k+1}). \quad (3)$$

If $q_{\text{init}}(i, t_k)$ is independent of time, $q_0(i, t_{k+1}) = q(i, 0)$, that is, the initial condition of the conventional mechanism. Note that, in general, we allow the time-dependence of $q_{\text{init}}(i, t_k)$. Next, for $q_{n+1}(i, t_{k+1})$ ($n = 0, 1, \dots, N - 1$), we set

$$q_{n+1}(i, t_{k+1}) = \mathcal{T}(q_n(i-1, t_k), q_n(i, t_k), q_n(i+1, t_k)). \quad (4)$$

Although the above rule may look complicated, we can easily understand it through graphical representation. Figure 2 explains the temporal evolution of vector (2) at node i . The horizontal axis represents discrete time as t_0, t_1, \dots , and $q_{\text{init}}(t_k)$ is a certain value expressing the network state of a node at time t_k . Each component of the vector is a value of the distribution and (4) is the temporal evolution rule for the n th component ($n = 1, 2, \dots, N - 1$). The temporal evolution of each component will be updated to the upper-right component in Figure 2. The component at the bottom, $q_0(i, t_{k+1})$, is overwritten by the network condition $q_{\text{init}}(i, t_{k+1})$ at the present time. The component at the top will be discarded.

The temporal evolution of the conventional mechanism corresponds to the sequence indicated by the green broken line in Figure 2. In the guarantee mechanism of asymptotic stability, we focus on the sequence of the same vector components. If we choose small n for the n th component, we obtain a finer-grained spatial structure as indicated by the blue line. A large n yields a coarse grained spatial structure as indicated by the red line.

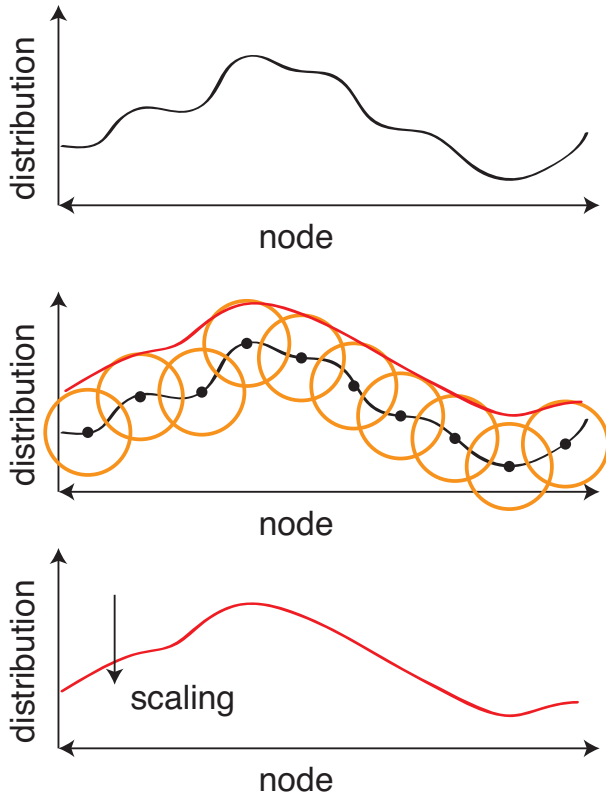


Figure 4. Renormalization transformation as per Huygens' principle.

III. DESIGN OF THE AUTONOMOUS STRUCTURE FORMATION TECHNOLOGY BASED ON HUYGENS' PRINCIPLE

In this section, we first propose a new autonomous decentralized clustering based on Huygens' principle and its renormalization transformation. Second, we investigate the attenuation of the cluster structure caused by the fixed point of the renormalization transformation, and introduce a procedure of amplification for avoiding the attenuation.

A. Huygens' principle and Renormalization

Huygens' principle, or the Huygens-Fresnel principle describes the temporal evolution of the wavefront and can explain the laws of reflection and refraction. Figure 3 shows an example of wave propagation obeying Huygens' principle. Let us consider a wavefront at present time t . In Huygens' principle, spherical waves originate from all points on the wavefront and the envelope of these spherical waves gives the temporal evolution of the wavefront at time $t + \Delta t$.

Renormalization is a way to extract simple and important macroscopic characteristics from a large-scale and complex system, and its procedure is called renormalization transformation. This procedure is suitable for generating a simple cluster structure extracted from the spatial structure of the network state. Renormalization transformation is defined as the combination of coarse-grained transformation and scaling. In this paper, we adopt the renormalization transformation based on Huygens' principle as temporal evolution operation

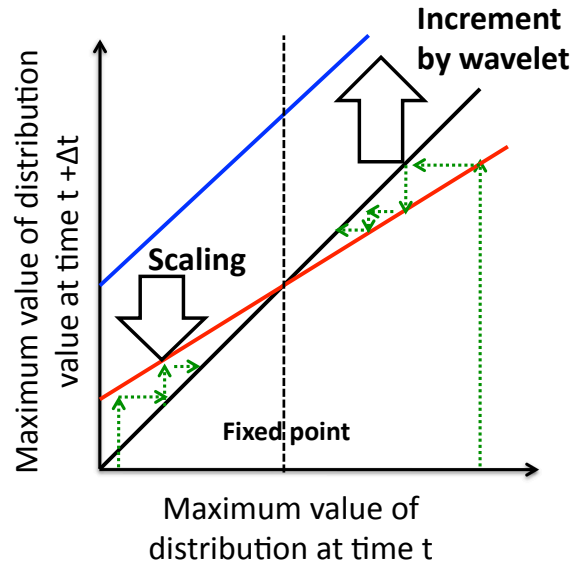


Figure 5. Fixed point under renormalization transformation.

\mathcal{T} . Specifically, each node generates spherical wave-like information for temporal evolution of the distribution. Concrete procedures of the renormalization transformation are shown below.

Let us consider a one-dimensional network and a distribution on the network. The panel at the top of Figure 4 shows an example of the distribution at the present time. We consider the shape of the distribution as the wavefront. The panel at the middle of Figure 4 shows the temporal evolution of the wavefront as given by Huygens' principle. This procedure has a smoothing effect in which the fine-grained structure in the shape of the distribution becomes smooth. The temporal evolution of the distribution causes an increase in the value of the distribution, that is, the wavefront proceeds upward. In order to compensate for this increase, we introduce scaling as shown in the panel at the bottom of Figure 4. We define the renormalization transformation as the combination of such temporal evolution and scaling.

Let the distribution value of node i at time t_k be $q(i, t_k)$, and let the set of nodes that are adjacent to node i at time t_k be $M(i, t_k)$. In addition, $\tilde{q}(i, j, t_{k+1})$ is the wavefront of the spherical wave at node i at time t_{k+1} that originated from node j at time t_k . Our renormalization transformation is expressed as

$$q(i, t_{k+1}) = \frac{1}{b} \max_{j \in M(i, t_k)} \tilde{q}(i, j, t_{k+1}), \quad (5)$$

where, the maximizing operation in (5) means Huygens' principle; it determines the most advanced wavefront of spherical waves that originated from the node itself and its neighborhood, b is the scaling parameter.

Next, let us consider a method of tuning parameter b using Figure 5. In Figure 5, the horizontal axis represents the maximum value of the distribution at time t , and the vertical axis represents the maximum value of the distribution after renormalization transformation at time $t + \Delta t$. Here, the black

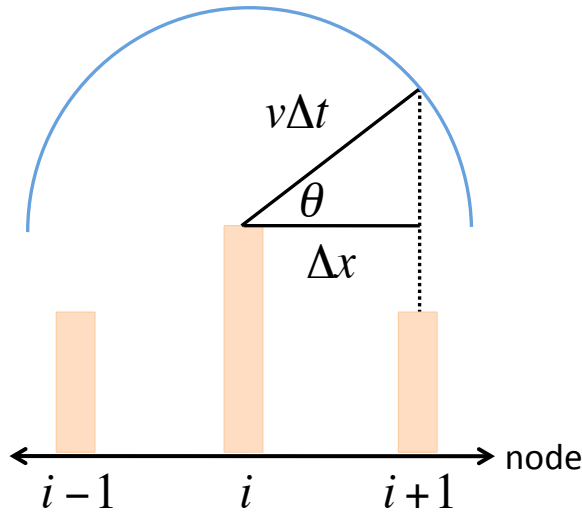


Figure 6. The wavefront of the spherical wave reaches an adjacent node.

line shows the linear equation $y = x$. This linear equation corresponds to the top of Figure 4. Next, the maximum value of the distribution is increased obeying Huygens' principle. This increment can be expressed by $v\Delta t$ and the blue line, which is shifted up from $y = x$ by $v\Delta t$. The red line is obtained from the blue line by dividing the latter by the scaling parameter b ($b > 1$). There is an intersection point between the red line and the black line, and this intersection point is given by

$$p^* = \frac{v\Delta t}{b-1}. \quad (6)$$

The value of interaction point p^* is the fixed point under renormalization transformation. We can understand that the maximum value of distribution $q(i, t_k)$ converges to p^* with iterations of the temporal evolution, regardless of initial condition $q(i, 0)$. Hence, the method of tuning parameter b does not need to be highly accurate.

Next, we consider the concrete form of $\tilde{q}(i, j, t_{k+1})$. Let the propagation speed of the spherical wave be v , the distance between two adjacent nodes be Δx , and the interval of the temporal evolution (renormalization transformation (5)) be Δt (i.e., $t_{k+1} - t_k = \Delta t$). Here, Δx is not physical distance but is a kind of hop count, so we choose $\Delta x = 1$. We consider the situation wherein the temporal evolution (5) is determined only by adjacent nodes, v is chosen as $1 \leq v\Delta t < 2$. As shown in Figure 6, the wave front of the spherical wave originating from node i influences both node i and its adjacent nodes. They are expressed as

$$\tilde{q}(i \pm 1, i, t_{k+1}) = q(i, t_k) + v\Delta t \sin \theta, \quad (7)$$

$$\tilde{q}(i, i, t_{k+1}) = q(i, t_k) + v\Delta t, \quad (8)$$

where θ is a constant and, from $v\Delta t \cos \theta = \Delta x$,

$$\theta = \arccos \left(\frac{\Delta x}{v\Delta t} \right). \quad (9)$$

Since v , Δt , and $\sin \theta$ are constants and we can know them in advance, temporal evolution (5) is a simple operation.

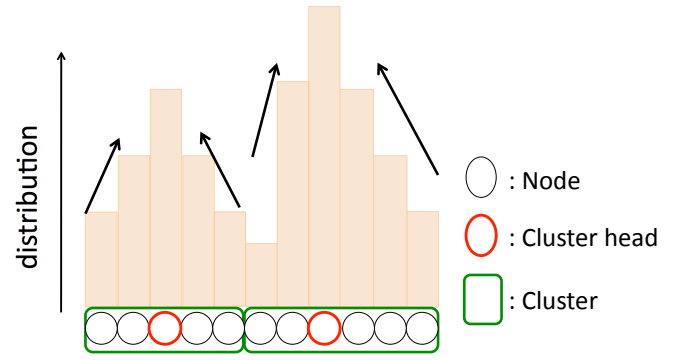


Figure 7. Determination of the cluster and cluster head.

B. Amplification of the Range of the Distribution

Our renormalization transformation (5) makes the distribution flat and we can obtain a coarse-grained spatial structure. However, different from physical phenomena, there are situations that the distribution does not change when the difference in distribution values is small. This is because the positions of nodes in the network are discrete. If the distribution value at a node can affect that of the adjacent node, the following relation is required;

$$|q(i \pm 1, t_k) - q(i, t_k)| > v\Delta t (1 - \sin \theta). \quad (10)$$

When smoothing proceeds and the condition (10) is no longer met, the two adjacent nodes no longer interact and the distribution is unchanged. To avoid this phenomenon, we introduce amplification of the range of the distribution in addition to renormalization transformation (5). The additional operation is

$$q(i, t_{k+1}) \leftarrow p^* + a (q(i, t_{k+1}) - p^*), \quad (11)$$

after renormalization transformation (5). This operation means that the difference between the distribution value and p^* is amplified by a factor of a . Here, the aforementioned $p^* = v\Delta t/(b-1)$ is the fixed point of renormalization transformation, and also is the convergence point. Note that, the value of parameter a should be chosen as $a > b$.

Finally, we explain how to determine clusters and cluster heads from the generated spatial structure (Figure 7). By following the direction of the steepest gradient of the distribution, we can find a node with local maximum value. We define it as the cluster head, and the nodes belonging to the same cluster head belong to the same cluster.

IV. EVALUATION FOR STATE DEPENDENT CHARACTERISTICS OF CLUSTERS

This section shows cluster structures generated by our proposed scheme using numerical examples and verifies that they reflect the network condition. Our simulation programs are written by C language.

A. Simulation Model and Parameters

In this subsection, we explain a simulation model and parameters used in our verification. In this verification, we use a unit disk graph having a torus boundary as the network model.

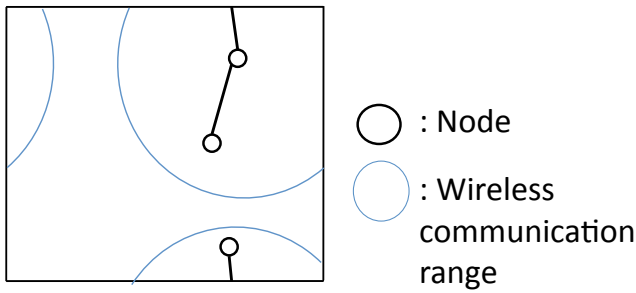


Figure 8. Unit disk graph having torus boundary.

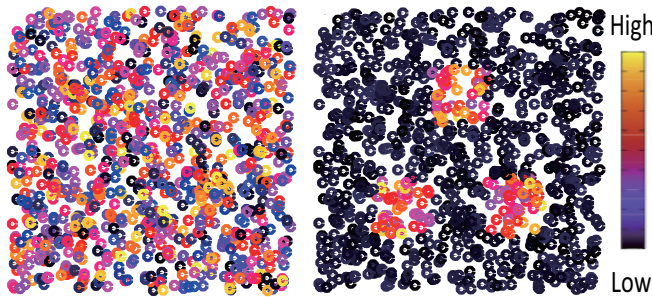


Figure 9. Initial condition.

We can configure the unit disk graph through the following procedure. We set the position of each node randomly, and set a circle of a certain radius around each node. If the circle of a node encloses another node(s), we set a link between the center node of the circle and each node lying within the circle. Since we can assume that circle radius is wireless communication range, the unit disk graph is a model that can express MANET topology. Figure 8 shows an example of the torus boundary by focusing on the wireless communication range of a certain node. The reason of setting the torus boundary condition is to eliminate the effect of the network edge, and to concentrate our attention on the characteristics of clustering mechanism itself. In this evaluation, we set 1,000 nodes on a plane of $1 \text{ km} \times 1 \text{ km}$, and use 60 m as the wireless communication range.

In order to verify the state dependent characteristics of the cluster structures generated, we use two initial distributions as shown in Figure 9 where distribution values are described by a color map. The left figure in Figure 9 expresses a randomized state. The initial values of $q_{\text{init}}(i, 0)$ for all node positions, i , are random values that obey a uniform distribution with range $[0, 10]$. The right figure in Figure 9 expresses a spatially structured state. Three areas have relatively high values, and the values of these areas are determined by random values that obey a uniform distribution with range $[5, 10]$. The values of other area are determined by random values that obey a uniform distribution with range $[1, 2]$. If, for example, the value represents battery energy, the randomized state does not express any power-supply information whereas the spatially structured state indicates three power-supply zones. The parameters used in the evaluation are shown in Table I.

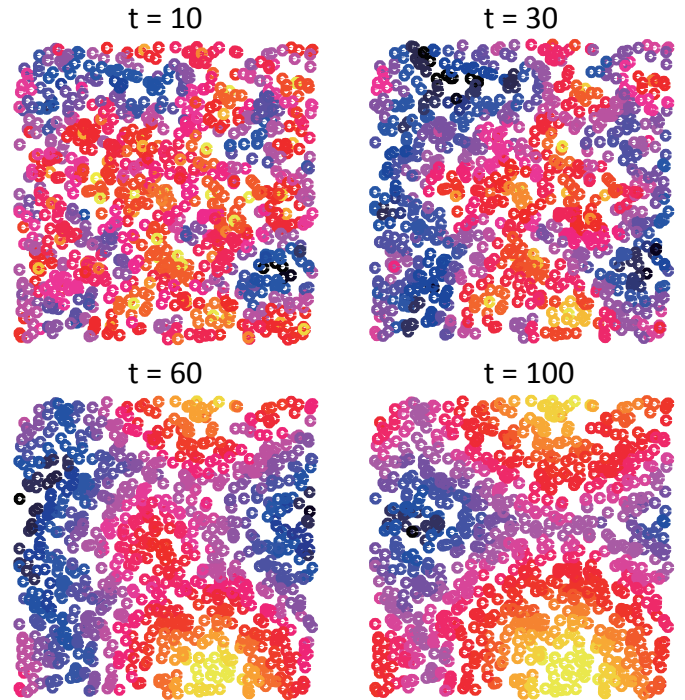


Figure 10. The cluster structures generated from a randomized state.

B. Evaluation

Figures 10 and 11 show the cluster structures generated from a randomized state and a spatially structured state, respectively. The four panels of each figure shows the number of iterations or, equivalently, the position of the vector component in the guarantee mechanism of the asymptotic stability of cluster structures. From these results, if we choose few iterations, we get a finer-grained cluster structure, and if we choose more iterations, we get a coarse grained cluster structure. We can also recognize that the cluster structures reflect the spatially configured state of the initial condition. Since the initial condition reflects the network state (e.g., battery power of each node), it means the cluster structure generated by our proposed scheme can reflect the state information of the network.

V. CONTROLLABILITY OF THE NUMBER OF CLUSTERS BASED ON THE GUARANTEE MECHANISM OF ASYMPTOTIC STABILITY

This section investigates the clusters generated by our proposed scheme combined with the guarantee mechanism of asymptotic stability and reveals a technological problem

TABLE I. PARAMETER SETTING.

parameter	value
v	1.5
b	1.1
a	1.2
Δx	1.0
Δt	1.0

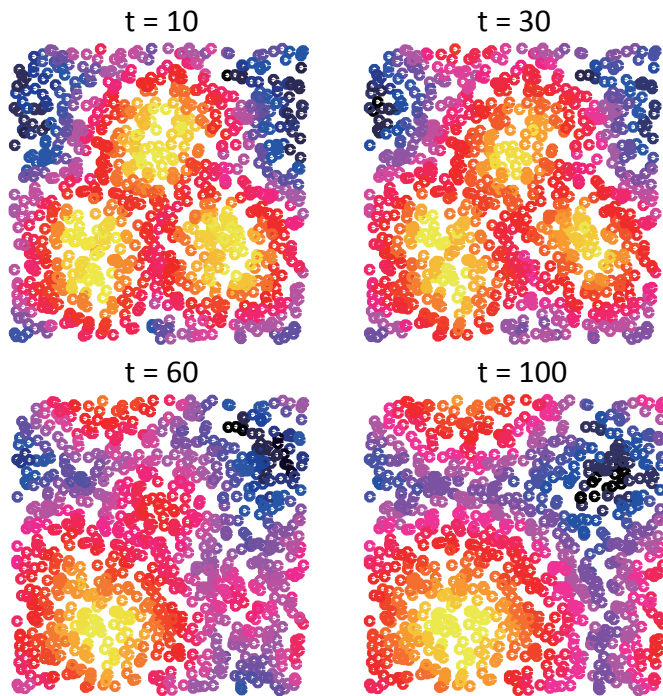


Figure 11. The cluster structures generated from a spatially structured state.

for ensuring control of the number of clusters. To solve this problem, we propose a control method of the number of clusters by introducing a logarithmic representation of network state.

A. Metric for Describing Network State

Let us consider what metrics can be used to describe network state. For example, we can use node battery power as the initial condition of nodes that reflects the state of the network. There are many ways to express the battery power in numerical values: ampere-hour [Ah], milli-ampere hour [mAh], coulomb [C], etc. Incidentally, $1 \text{ Ah} = 1,000 \text{ mAh} = 3,600 \text{ C}$. Thus, the ranges of the initial distribution may quite different depending on the metric used, even if the target networks are in the same environment. In addition, it is possible that some other network state metrics might be included as a part of the distribution value. Therefore, it is difficult to specify the metric for describing network state in advance.

In our proposed clustering scheme combined with the guarantee mechanism of asymptotic stability, the number of clusters are controlled by choosing the number of iterations (i.e., the position of the vector component of (2)). In order to realize the control of the number of clusters based on our framework, for any given iteration number, the number of generated clusters should be independent of the metric.

B. Evaluation for Dependence Characteristics on the Range of the Initial Distribution

In this subsection, we investigate the convergence of the number of generated clusters with respect to the range of

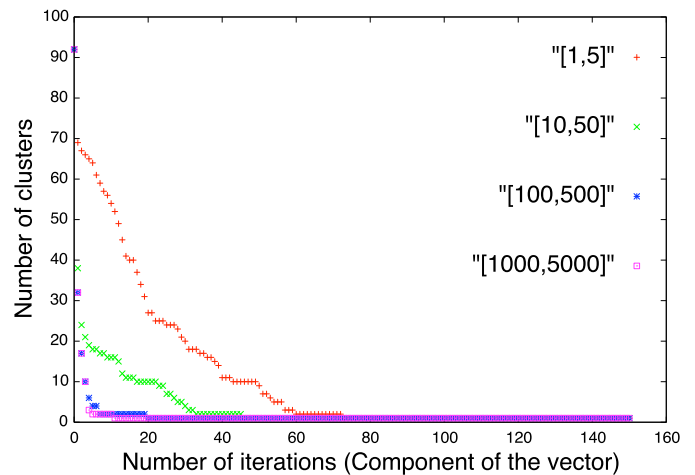


Figure 12. The number of generated clusters for randomized initial conditions w.r.t. the number of iterations.

the initial distributions. We use the same network model and parameter setting as used in the previous section. The values of the initial distribution $q_{\text{init}}(i, 0)$ for all node positions, i , are given by a random values that obey a uniform distribution; four kinds of uniform distributions are examined. Their ranges are $[1, 5]$, $[10, 5 \times 10]$, $[10^2, 5 \times 10^2]$ and $[10^3, 5 \times 10^3]$. The difference in ranges means the difference in the metrics. An example of an initial condition is shown in the left pane of Figure 9.

Figure 12 shows the temporal evolutions of the number of clusters obtained from four different initial conditions. From these results, we can recognize that the number of clusters strongly depends on the range of the initial distribution. Also, the relationship between the number of clusters and the iteration times depends on the range of the initial distribution. Since we cannot know the network state and its metric in advance, we cannot control the number of clusters.

The cause of the above problem is the excessive sensitivity of cluster formation to the range of the distribution. The mechanism of the excessive sensitivity with respect to the range of the distribution can be recognized through Figure 13. Figure 13 shows the behaviors of cluster formation obtained from our proposed scheme for the initial distributions with large and small ranges. First, each node performs temporal evolution obeying Huygens' principle, and then scaling. Small-valued nodes, which are next large-valued nodes, are greatly influenced by the latter, and the difference in values between them is strongly decreased. Therefore, if the range of the initial distribution is large, the distribution is rapidly harmonized.

C. Proposal of Control Method of the Number of Clusters

In order to avoid the problem caused by the difference in the ranges of distribution, we redefine the initial condition. The details are as follows. We do not use the network condition directly as the initial condition, but instead use

$$q(i, 0) = \log(q_{\text{init}}(i, 0)). \quad (12)$$

In the vector formulation, we replace (3) with

$$q_0(i, t) = \log(q_{\text{init}}(i, t)). \quad (13)$$

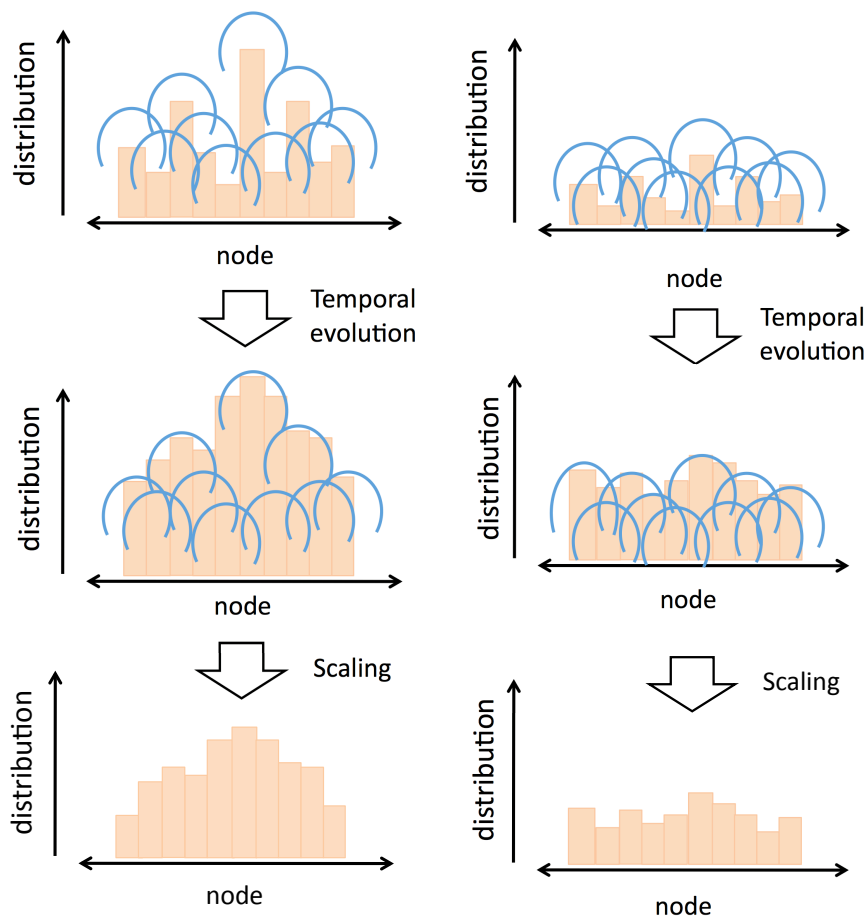


Figure 13. An example of the behavior of the proposed mechanism on two different distribution ranges.

The reasons for introducing a logarithmic function are as follows:

- It is possible to maintain the magnitude relation of the values of the original initial distribution.
- If the value of the original initial distribution is large, its new equivalent value is smaller in the sense of the ratio.

Let us consider the situation wherein the range of initial condition is given by $[Ax, Bx]$. Where x is a positive constant representing the difference between metric values. Here, we define the distribution range function $R[q]$ as the difference between the maximum and minimum values of distribution q . The range of the conventional distribution, q_{init} , is expressed as follows:

$$R[q_{init}] = (B - A)x. \quad (14)$$

This means that the range of the distribution depends on x . On the other hand, the range of the new distribution $\log q_{init}$ is expressed as follows:

$$R[\log(q_{init})] = \log(Bx) - \log(Ax) = \log\left(\frac{B}{A}\right). \quad (15)$$

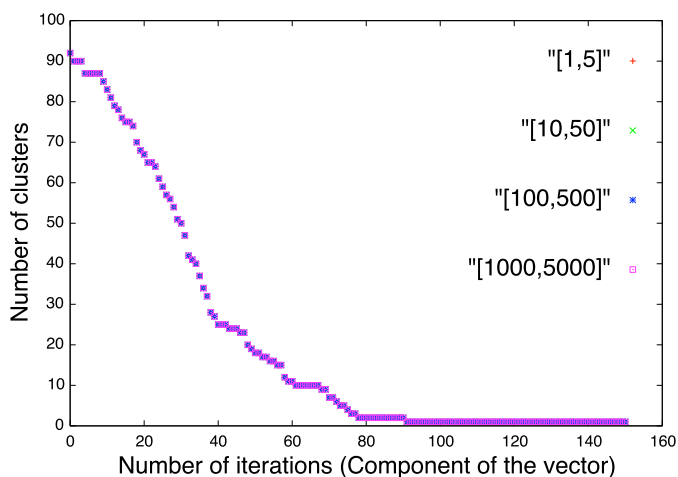


Figure 14. The number of clusters generated using logarithmic function from randomized initial conditions, w.r.t. the number of iterations.

This means that the range of the distribution is independent of x . It also means that the range of the redefined initial distribution is independent of the metric used.

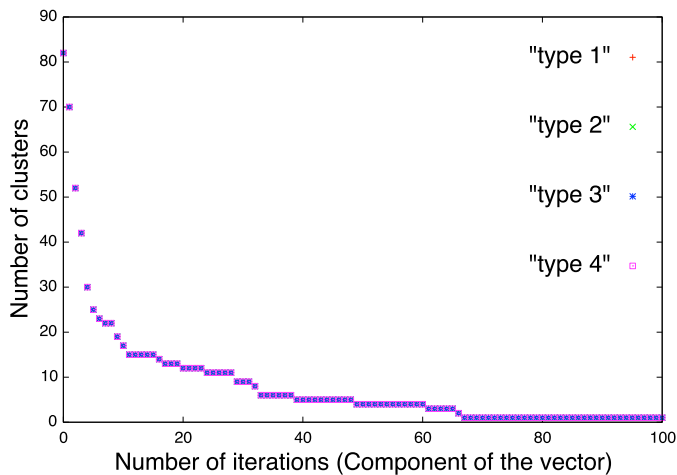


Figure 15. The number of clusters generated using logarithmic function from the initial condition having patterned structure, w.r.t. the number of iterations.

D. Evaluation for Controllability of the Number of Clusters

Figure 14 shows similar evaluations to Figure 12 by using the redefined initial condition (13). We recognize that the impact of the initial condition is sufficiently weakened. In particular, all initial conditions yield completely the same result. This means that we have a robust clustering mechanism that can control the number of clusters by appropriately choosing the number of iterations or the component of the vector.

Next, we evaluate an effectiveness of our control method on other type of initial distribution. We use the initial distribution having spatially structured state (right figure in Figure 9). Also, we prepare the range of initial conditions in the same manners as the previous evaluation. Specifically, their ranges are as follows. The values on the three areas are determined by random values that obey a uniform distribution with range [5, 10]. The values on the other areas are also determined by random values that obey a uniform distribution with range [1, 2]. Let us call this initial condition type 1. Next, we define the initial condition type 2, whose ranges are calculated by raising the ranges of type 1 by a factor of ten. In the same manner, we define type 3 and type 4.

Figure 15 shows the temporal evolution in the number of clusters obtained from our scheme with the logarithmic initial conditions for the four different ranges. From these results, we can recognize that the number of clusters is independent of the range of initial distribution even if the initial distribution is spatially structured. Therefore, our proposed scheme can be expected to control the number of clusters even if the initial distribution has a complex spatial structure.

VI. CONCLUSION AND FUTURE WORK

In this paper, we proposed an autonomous clustering mechanism based on Huygens' principle for MANETs. For verification, we used a unit disk graph to evaluate the characteristics of the proposed scheme. The benefits of the proposed algorithm lie in its simplicity and its ability to form the spatial structure reflecting the initial condition of network states. To control the number of clusters generated, the number should

be independent of the metric representing the initial network condition. However, unfortunately, the convergence speed of cluster configuration depends strongly on the range of the initial distribution that describes the network state. Since we cannot know the distribution value for each node in advance, the difference in convergence speed makes it impossible to control the number of clusters. To avoid this problem, we introduced new distribution defined by the logarithm of the original distribution. Consequently, the difference in convergence speed is significantly weakened, and the number of clusters becomes controllable. The above characteristics are suitable for clustering in MANET. As future work, we will consider the response of our mechanism to dynamic environments.

ACKNOWLEDGMENT

This work was supported by a Grant-in-Aid for Scientific Research (B) No. 23300031 (2011-2013) from the Japan Society for the Promotion of Science.

REFERENCES

- [1] Kenji Takagi, Masaki Aida, Chisa Takano, and Makoto Naruse, "A proposal of new autonomous decentralized structure formation based on Huygens' principle and renormalization," in Proceedings of the 3rd International Conference on Advanced Collaborative Networks, Systems and Applications (COLLA 2013), Jul. 21–26, 2013, Nice, France, pp. 75–80, ISBN: 978-1-61208-287-5, ISSN: 2308-4227.
- [2] Charles E. Perkins, Ad Hoc Networking, Addison-Wesley, Jan. 2001, ISBN: 978-0201309768.
- [3] Charles E. Perkins, Elizabeth M. Belding-Royer, and Samir R. Das, "Ad hoc on-demand distance vector (AODV) routing," Request for Comments 3561, Jul. 2003.
- [4] Yu-Chee Tseng, Sze-Yao Ni, Yuh-Shyan Chen, and Jang-Ping Sheu, "The broadcast storm problem in a mobile ad hoc network," Wireless Networks, Kluwer Academic Publishers, vol. 8, issue 2–3, Mar. 2002, pp. 153–167, ISSN: 1572-8196.
- [5] Josh Broch, David A. Maltz, David B. Johnson, Yih-Chun Hu, and Jorjeta Jetcheva, "A performance comparison of multi-hop wireless ad hoc network routing protocols," in Proceedings of MOBICOM'98 of the 4th annual ACM/IEEE international conference on Mobile computing and networking, Oct. 25–30, 1998, Dallas, TX, USA, pp. 151–162, ISBN: 1-58113-142-9.
- [6] Stefaan Seys and Bart Preneel, "ARM: Anonymous routing protocol for mobile ad hoc networks," International Journal of Wireless and Mobile Computing, Inderscience Publishers, vol. 3, issue 3, Oct. 2009, pp. 145–155, ISSN: 1741-1084.
- [7] Stefano Basagni, "Distributed clustering for ad hoc networks," in Proceedings of the 4th International Symposium on Parallel Architectures, Algorithms, and Networks, 1999 (I-SPAN'99), Jun. 23–25, 1999, Perth/Fremantle, WA, USA, pp. 310–315, ISSN: 1087-4089.
- [8] Tomoyuki Ohta, Shinji Inoue, Yoshiaki Kakuda, and Kenji Isida, "An adaptive multihop clustering scheme for ad hoc networks with high mobility," IEICE Transactions on Fundamentals, vol. E86-A, no. 7, Jul. 2003, pp. 1689–1697, ISSN: 0916-8508.
- [9] Giovanni Neglia and Giuseppe Reina, "Evaluating activator-inhibitor mechanisms for sensors coordination," in Proceedings of the 2nd IEEE/ACM International Conference on Bio-Inspired Models of Network, Information and Computing Systems (Bionetics 2007), Dec. 10–12, 2007, Budapest, Hungary, pp. 129–133, ISBN: 978-963-9799-05-9.
- [10] Masaki Aida, "Using a renormalization group to create ideal hierarchical network architecture with time scale dependency," IEICE Transactions on Communications, vol. 95-B, no. 5, May 2012, pp. 1488–1500, ISSN: 0916-8516.
- [11] Chisa Takano, Masaki Aida, Masayuki Murata, and Makoto Imase, "New framework of back diffusion-based autonomous decentralized control and its application to clustering scheme," in Proceedings of the IEEE Globecom 2010 Workshop on the Network of the Future

- (FutureNet III), Dec. 6–19, 2010, Miami, FL, USA, pp. 362–367, ISBN: 978-1-4244-8863-6.
- [12] Chisa Takano, Masaki Aida, Masayuki Murata, and Makoto Imase, “Proposal for autonomous decentralized structure formation based on local interaction and back-diffusion potential,” *IEICE Transactions on Communications*, vol. E95-B, no. 5, May 2012, pp. 1529–1538, ISSN: 0916-8516.
- [13] Ryo Hamamoto, Chisa Takano, Kenji Ishida, and Masaki Aida, “Guaranteeing asymptotic stability of clustering by autonomous decentralized structure formation,” in *Proceedings of the 9th IEEE International Conference on Autonomic and Trusted Computing (ATC 2012)*, Sep. 4–7, 2012, Fukuoka, Japan, pp. 408–414, ISBN: 978-1-4673-3084-8.
- [14] Kenji Takagi, Yusuke Sakumoto, Chisa Takano, and Masaki Aida, “On convergence rate of autonomous decentralized structure formation technology for clustering in ad hoc networks,” in *Proceedings of the 32nd International Conference on Distributed Computing Systems Workshops (ADSN 2012)*, Jun. 18–21, 2012, Macau, P.R.China, pp. 356–361, ISBN: 978-1-4673-1423-7, ISSN: 1545-0678.
- [15] Hiroki Takayama, Sota Hatakeyama, and Masaki Aida, “Self-adjustment mechanism guaranteeing asymptotic stability of clusters formed by autonomous decentralized mechanism,” *Journal of Communications*, vol. 9, no. 2, Feb. 2014, pp. 180–187, ISSN: 1796-2021.